CORROSION SCIENCE AND TECHNOLOGY, Vol.24, No.5(2025), pp.309~318 pISSN 1598-6462 / eISSN 2288-6524
[Research Paper] DOI: https://doi.org/10.14773/cst.2025.24.5.309

Cerium (III) Oxide – Based Conversion Layer on Galvanized Steel: Preparation and Inhibition Properties Characterization

Thuy Duong Nguyen[1], Viet Phuong Nguyen[2], Ai Nhi Pham Thi[2], Thuy T.B. Hoang[2], Anh Truc Trinh[1], and Thu Thuy Thai[1,†]

[1]*Institute of Materials Science, Vietnam Academy of Science and Technology, A13 Building, 18 Hoang Quoc Viet, Nghia Do, Hanoi, Vietnam*
[2]*School of Chemistry and Life Sciences, Hanoi University of Science and Technology, 1 Dai Co Viet, Hanoi, Vietnam*

(Received November 25, 2024; Revised December 31, 2024; Accepted January 1, 2025)

This study presents inhibitive protection of commercial cerium (III) oxide (Ce_2O_3) for a galvanized steel substrate in a corrosive solution. Electrochemical measurements revealed that Ce_2O_3 at a small content (0.05 wt%) had an inhibitor capacity by forming a protective layer after a short immersion. The morphology and growth of the Ce-rich passive film were subjected to field-emission scanning electronic microscopy (FE-SEM) and x-ray diffraction (XRD) analysis. Results showed round-shaped crystals mainly composed of zincite, simonkolleite, and cerium carbonate. Polarization curves confirmed the inhibitory action of Ce_2O_3 as a cathodic inhibitor. The cerium (III) oxide was then used as the main composition to prepare a cerium-based conversion layer on a galvanized steel substrate, presenting a homogenous and crystal-shape structure revealed by FE-SEM and EDS analysis. This cerium pretreatment layer can help reinforce the adhesion performance (approved by ASTM D4541 pull-off test standard) and anti-corrosion properties (approved by ASTM B117 salt spray test standard) between the epoxy layer and the galvanized steel substrate.

Keywords: *Galvanized steel, Corrosion, Cerium oxide, Cerium conversion layer, Adhesion*

1. Introduction

The chromium hexavalent (Cr (VI)) compounds have been known as the most effective inhibitors for many types of common metallic substrates as aluminum alloy, carbon steel, zinc-based alloy surface [1,2]. The Cr (VI) compounds show their applications not only in organic, inorganic or hybrid coatings but also in metallic production like pretreatment or the passivation before commercial purchase. From the 1988s, the replacement of Cr (VI) products started becoming the urgent requirements. In this state, the research on the cerium compounds has become one of the new trends in the anticorrosion protection industry.

Zn-based metallic substrates, especially galvanized steels retain a positive effect in neutral medium as a consequence of the sacrificial protective of zinc coating on the top. Moreover, when working in aggressive environment, galvanized steel is responsive to be corroded [3,4]. As the result, the inhibitive influence of cerium compounds receives the increasing attention to prolong the lifetime of galvanized steel components [3,5-7]. Although the protective mechanism is still under discussion, but the researchers agree that this action of cerium compounds is based on the reactions at the cathodic zone, linking to the precipitation of insoluble products (cerium hydroxides/ cerium oxides) at high pH localized areas, thereby reducing the dissolution of zinc at the anodic sites so reducing the corrosion rate [3,8].

The protective effect of cerium has been proved in various applications. In the solution, Aramaki et al. studied the inhibitive effect of cerium chloride when immersed the zinc substrate in the 0.1 M NaCl solution [3]. A passivated layer was formed on the Zn surface which included $Ce(OH)_3$, $Zn(OH)_2$ and ZnO compounds that slow down the corrosion process. This phenomenon was also approved by the study of Arenas et al [9] that confirming the formation of a yellow insoluble layer on

[†]Corresponding author: ttthuy@ims.vast.ac.vn

the hot dip galvanized steel surface after 4 hour of immersion in the 3.5 wt% NaCl solution containing the $CeCl_3$ in the range from 100 – 1000 ppm. In recent study, the two salts of cerium which were $CeCl_3$ and $Ce(NO_3)_3$ were examined in chloride solution for four different types of zinc-based metallic substrate, including hot dip galvanized steel (HDG) [5]. XRD results indicated the growth of simonkolleite $Zn_5(OH)_8Cl_2.(H_2O)$ on HDG surface not depending on the counter-ion (Cl^- or NO_3^-). Nevertheless, the nitrate anions reinforced the protective effect for the HDG steel higher than the chlorides ions due to the anodic effect of NO_3^-. These were also the two most common types of cerium salt (cerium chloride, cerium nitrate) that were reported in the literature.

In particular, cerium-based conversion coating is employed as a useful pretreatment method in replacement of the use of Cr (VI) compounds in processing bath. The main propositions are cerium salt and an oxidant (H_2O_2 normally) in acidic solution. The growth of the cerium surface treatment layer includes the oxidation reaction of the metal substrate and the reduction reaction of hydrogen peroxide [10,11]:

$$Zn \rightarrow Zn^{2+} + 2e^-$$
$$H_2O_2 + 2e^- \rightarrow 2OH^-$$

These reactions produce OH^- ions so resulting the increase in pH value at local sites, following the precipitation of Ce (IV) oxide:

$$Ce^{3+} + OH^- + 1/2\ H_2O_2 \rightarrow Ce(OH)_2^{2+}$$
$$Ce(OH)_2^{2+} + 2OH^- \rightarrow Ce(OH)_4$$
$$Ce(OH)_4 \rightarrow CeO_2 + 2H_2O$$

The objective of the pretreatment layer not only reinforces the corrosion properties of global protective system but also helps to increase the adhesion behavior with the upper organic layer. Moreover, there is a few of studies focused on the effect of the conversion layer with the organic coating [12,13], especially Ce-conversion layer. Mahidashiti et al reported the strengthening of the cerium nitrate-based conversion layer on the presence of an epoxy layer applied on steel [12]. When compared with the epoxy coating covered on untreated steel, the Ce-pretreatment layer/ epoxy system clearly shows the enhancement in the anticorrosion protection, resulting in the non-corrosion products at the surface after one thousand hours of salt spray test.

Besides the cerium salts, cerium oxide is also known as the potential inhibitor for steel and galvanized steel, mainly focused on cerium (IV) oxide [14,15]. Therefore, the cerium (III) oxide or dicerium dioxide – a rare earth cerium-compound has not yet received much attention, mostly used for catalyze the reduction of CO emissions from fuel combustion [16]. This study focuses on the corrosion inhibition effect of cerium (III) oxide on galvanized steel substrate and then formulate a surface treatment layer based on cerium (III) oxide that can reinforce the anti-corrosion protection ability and good adhesion to primer and metal substrate.

2. Experimental Methods

2.1 Materials

Cerium (III) oxide particles (≥ 98%) were purchased from Vietnam Rare Earth Joint Stock Company and used as received.

Galvanized steel sheets (40 × 60 × 1 mm) with 35-40 μm of zinc thickness layer were cleaned in acetone bath for 10 min, continued degreasing in NaOH solution (pH 12, 1 min, 50 °C) then cleaned in ethanol absolute [17]. For the aim of investigating the inhibition efficiency, the galvanized steel substrates were surrounded in epoxy resin in respect of the surface working area (4 cm^2) and to protect the edges samples in the corrosive medium.

2.2 Chemical conversion coating

A cerium-based conversion bath was prepared from 2 g/L of cerium (III) oxide and 0.6 ml/l of hydrogen peroxide (30 wt% in H_2O, Sigma Aldrich). The pH of solution was maintained at 2 (adjusted by HNO_3) and 3 (fixed by 5 wt% NaOH solution). After pre-cleaned, galvanized steel sheets were immersed in the cerium-based bath solution for 5 min at room temperature (25 ± 1 °C) then carefully rinsed by distilled water and dried.

2.3 Epoxy primer preparation

After cerium-conversion layer deposition, an epoxy layer was then continued depositing on pre-treated galvanized steel substrates. Epoxy Epotec YD 128 and Ancamine

2280 as hardener were prepared with the ration 2:1 including the mixture of xylene and butyl acetate (9/1 vol/vol) as solvent. The polymer mixture was stirred for 30 min then deposited on pretreated galvanized steel sheet by spin coating technique (Filmfuge Paint Spinner Ref 110N spin-coater) at 350 ppm of rotating rate for 10 s (room temperature). The dry film thickness was about 35 ± 5 µm, detected by Minitest 600 (Erichsen) coating thickness digital meter.

2.4. Characterization techniques

The X-ray diffraction (XRD) was performed by D8 Advance (Bruker) diffractometer set up with a Cu Kα emission source for cerium (III) oxide particles and the corrosion products formed on galvanized steel substrate after the inhibition test.

The surface morphology of galvanized steel sample after immersion in inhibitor-contained solution was observed by FE-SEM S-4800 Hitachi Field Emission Scanning Electronic Microscope equipped with an Energy Dispersive X-Ray spectrometer analysis (EDS). The surface of Ce-based conversion layer on galvanized steel was observed by digital microscope Keyence VHZ-100.

The electrochemical measurements were performed using Biologic VSP-300 potentiostat equipment with three-electrodes system. For this purpose, the Ag/AgCl/saturated KCl electrode (REF) was used as reference electrode while the Pt plate was used as counter electrode. For the inhibitor efficiency test of cerium (III) oxide, the working electrode made of galvanized steel (4 cm^2 of exposed area) as was immersed in the mixture of 0.05 M NaCl + 0.1 M Na_2SO_4 solution containing cerium (III) oxide at various concentration (0.03, 0.05 and 0.1 wt%). The EIS measurement was run out in the frequency range of 10 kHz to 10 mHz with the oscillation of 10 mV amplitude, 6 points per decade. The polarization curves were performed after the EIS measurement with the scan rate of 0.2 mV/s starting from the open circuit potential (OCP) versus cathodic or anodic direction (± 300 mV). At least three measurements were recorded to ensure the duplication of results.

The gloss retention of the galvanized steel surface pretreated in cerium-based solution was evaluated by BYK-Gardner AG-4446 Micro Tri-Gloss Meter according to ASTM E284-17 standard. The adhesion performance of epoxy layer/Ce-based conversion coating on galvanized steel surface was characterized by pull-off adhesion method followed the ASTM D4541 standard. The salt spray test of the double layer on galvanized steel was operated followed the B117 standard. Before set up in an accelerated salt spray chamber, an X cut (2 cm in length) was made on the surface as artificial default. The cut was verified by digital microscope to assure that the scratch cut through the protective layer reaching the metallic substrate.

3. Results and Discussion

3.1 Inhibitive effect of cerium (III) oxide for galvanized steel substrate

Fig. 1 presents the XRD pattern and zeta distribution

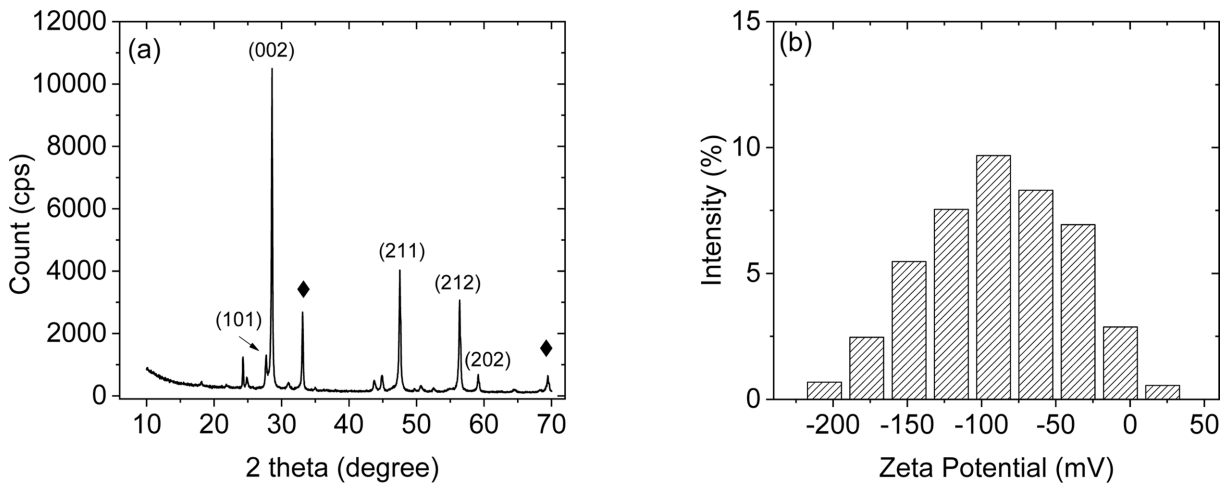

Fig. 1. XRD pattern (a) and zeta potential distribution (b) of cerium (III) oxide particles

of the investigated dicerium trioxide particles. As can be found in the literature (ID: mp-2721), the peaks in Fig. 1a related to the featured space of crystalline cerium (III) oxide particle as 27.9° (101), 28.9° (002), 47.5° (211), 56.5° (212); 59.0° (202), indicating the high purity of cerium (III) oxide. It also appeared the peaks corresponded to the CeO_2 traces (JCPDS: 34-0394) as 32.3° (200), 69.3° (400) indicating the phase transition between the dicerium trioxide and the cerium dioxide [16]. In addition, the zeta potential distribution (Fig. 1b) shows a distribution mainly in the negative zone with a zeta potential average around -91.0 mV, meaning the cerium (III) oxide particles are stable without reactions in the aqueous medium.

Fig. 2 presents the Nyquist plot obtained for galvanized steel substrate after 1 hour of immersion in Ce-based electrolyte solution. The result recorded for the immersion in no-inhibitor solution is also exhibited for reference.

As can be observed, the Nyquist plot recorded for galvanized steel working electrode immersed in no-containing inhibitor solution shows two semi-circle: the well-defined semi-circle at high frequency zone is related to the formation of corrosion product while the ongoing-semi circle at low frequency can be attributed to the charge transfer process [5,17]. In the presence of cerium oxide, two semi-circles are observed for all inhibitor concentrations. The first one is localized to the formation of cerium-based protective layer that can be clearly observed by the development of the diameter semi-circle value compared to the one obtained for reference solution. This semi-circle diameter is raised with the increase of cerium oxide concentration, from 0 to 0.03 wt% and 0.05 wt% linking to the development of a formed Ce-based layer that can retard the attack of corrosive species [5]. But when continuing increasing to 0.1 wt%, the semi-circle diameter is significantly decreased, lower than the one obtained for 0.05 wt% of Ce compound. In this case, the Ce-rich layer is also created but due to the accumulation of dicerium trioxide on the surface metallic, the Ce-based film becomes more porous film that can not support the barrier effect [8]. To clarify this phenomenon, Fig. 3 shows the FE-SEM image of galvanized steel surface after 1 hour immersed in experimental solution and Fig. 4 presents the chemical surface characterization result examined by XRD method.

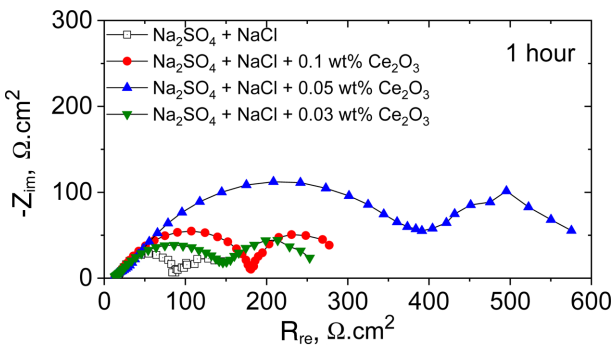

Fig. 2. Nyquist plot obtained for galvanized steel substrate immersed in electrolyte solution containing inhibitor after 1 hour of immersion

Concerning the surface morphology of corrosion products in Fig. 3, the crystal formation is completely different depending on the presence of inhibitor. After immersion in the blank solution (Fig. 3a), the galvanized steel surface shows a porous structure relating to the

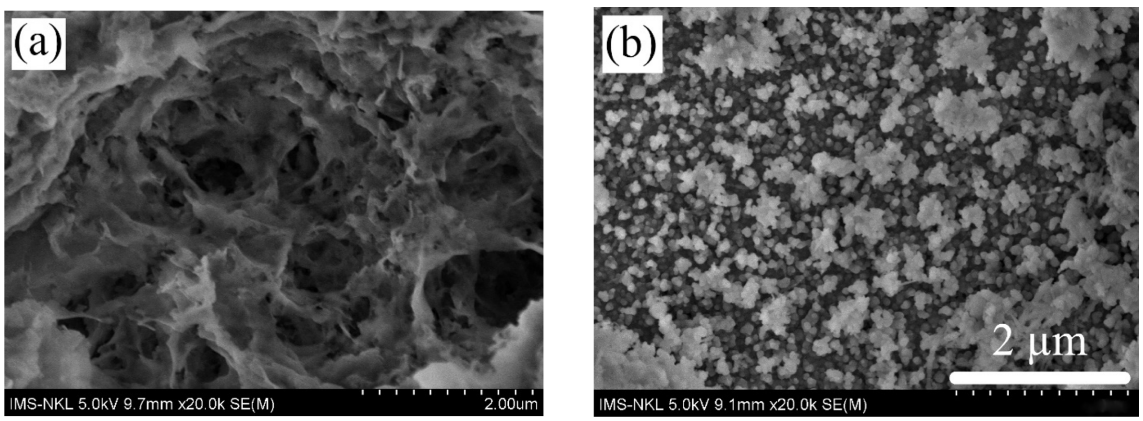

Fig. 3. FE-SEM observation of the galvanized steel after 1 hour of immersion in the electrolyte solution (a) and in electrolyte solution with 0.05 wt% Ce_2O_3 (b)

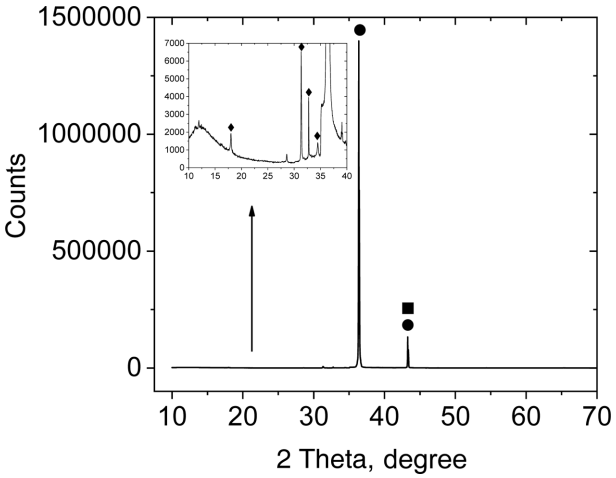

Fig. 4. XRD pattern of the galvanized steel substrate after 1 hour of immersion in the electrolyte solution with 0.05 wt% Ce_2O_3 (indicated in Fig. 3b). Peaks marked with ● related to the Zn, ■ linked to the $Zn_5(OH)_8Cl_2.H_2O$ and ♦ attributed to the $Ce_2(CO_3)_3 \cdot 6H_2O$ respectively

crystallization of zincite ZnO as mentioned in the literature [5,17,18]. In the presence of 0.05 wt% Ce_2O_3 in the solution, Fig. 3b respectively, a thicker layer is formed on the light-yellow- surface with a distribution of a round-shape crystal. This product covers all the surface with accumulations approving the formation of a protective layer that reduces the corrosion rate. Regarding the XRD results that analyzed this corrosion product (Fig. 4), the high intensity peak at 2θ close to the value of 36.4° is attributed to the zinc metallic, respectively. As can be observed, the peak at 43.3° can be corresponded to the zinc metallic but also the formation of simonkolleite as reported in the literature [5]. It is interesting when finding the formation of cerium carbonate (JCPDS No.00–030–0295) in the XRD pattern which identified at 18.2°, 31.3°, 33.1° and 34.7°. These peaks are respectively related to the (200), (060), (160), (161) characteristic space group of $Ce_2(CO_3)_3 \cdot 6H_2O$. The identification of cerium carbonate evidences the combination of cerium and carbonate species approving the formation of a cerium-rich film on the galvanized steel surface [9]. Although the short immersion (1 hour), the growth of inhibitive layer is developed and slowed down the attack of corrosive species. This helps to confirm the protective effect brought by the Ce_2O_3 that was discussed in the EIS measurement.

After EIS measurements, polarization experiments were taken place in order to approve the inhibitor ability of cerium (III) oxide. The polarization curves obtained after 1 hour of immersion of galvanized steel substrate in the Ce_2O_3-contained solution are shown in Fig. 5. The values of the current density corresponding to each solution are also reported in Table 1.

When considering the cathodic polarization curves (Fig. 5a), the corrosion potential E_{corr} obtained for the experiment in the no-inhibitor solution is around the value of -0.97 V (versus the potential of reference electrode). When adding the cerium (III) oxide particles, the E_{corr} is not changed depending on the increase of inhibitor content. Nevertheless,

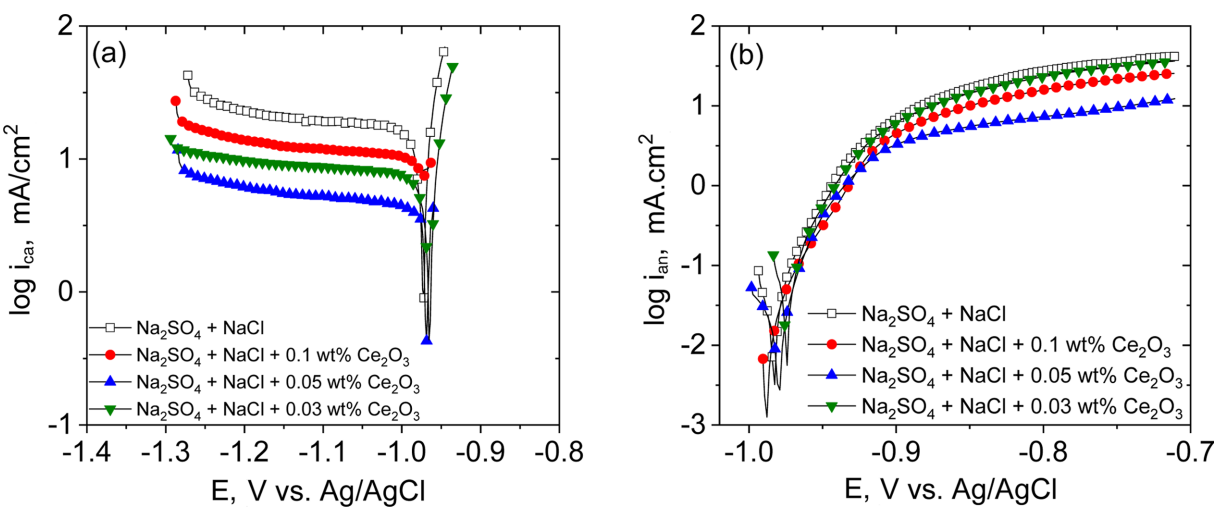

Fig. 5. Polarization curves obtained after 1 hour of immersion of galvanized steel surface in electrolyte solution containing cerium oxide

Table 1. The corrosion potential and the current density extracted from the polarization curves presented in Fig. 5

Solution	E_{corr} (V vs. Ag/AgCl)	i_{ca} (-150 mV versus E_{corr}) (mA/cm^2)
Na_2SO_4 + NaCl	-0.97	19.49
+ 0.03 wt% Ce_2O_3	-0.97	8.32
+ 0.05 wt% Ce_2O_3	-0.96	4.89
+ 0.1 wt% Ce_2O_3	-0.97	10.96

the current density has seemed to be decreased with the development of added cerium oxide, from blank solution to 0.03 wt% and 0.05 wt% Ce_2O_3. It must be noted that the current density obtained for the solution adding 0.05 wt% Ce_2O_3 is lower than 4 times of magnitude compared to the one recorded for the blank solution. This evolution of cathodic current density is similar to the first semi-circle diameter (as presented in Fig. 2) corresponding to the increase of the inhibitive effect of added pigment. It must be noted that when continued increasing the Ce_2O_3 content up to 0.1 wt%, the current density is increased, meaning that the high content of cerium oxide cannot support the protective effect for the galvanized steel substrate. Besides that, in the anodic polarization curves diagram presented in Fig. 5b, although the corrosion potential moves toward the cathodic direction in the presence of an inhibitor, the current density is un-changed. This can be concluded that the 0.05 wt% of Ce_2O_3 plays the role of cathodic inhibitor in order to protect the galvanized steel surface.

3.2 Ce-based conversion layer on the reinforcement of adhesion and anticorrosion properties on galvanized steel

Concerning the inhibition effectiveness of cerium (III) oxide for galvanized steel in the previous section, cerium (III) oxide particles are used as the main composition to prepare the cerium-based conversion layer. Two pH conditions are also examined. The surface appearances of galvanized steel substrate before and after pretreatment in 2 g/L cerium-based solution at pH 2 and pH 3 are exhibited in Fig. 6, which were taken by digital microscope (Fig. 6a, 6b, 6c) and by FE-SEM (Fig. 6b', 6c').

It can be remarked that before pretreatment, the galvanized steel sample initially shows a white-grey colour with some micro-cracks that can be clearly observed. This surface representation changes when being immersed in the cerium-containing solution that can be related to the formation of cerium-based layer at the metallic surface. When observed in Fig. 6b and Fig. 6c, the obtained surface shows some darken zones that can be linked to the dissolution of zinc and the acccumulation of Ce compound [9,11]. These reactions strongly happen in the solution more acidicity (pH 2) than the solution in pH 3, followed by a morphology more rugosity (Fig. 6b) than the other one (Fig. 6c) respectively. This is more evident when observed by FE-SEM, Fig. 6b' and Fig. 6c', that showing a homogenous surface morphology made by cerium immersion but the crystal shape is different depening on the pH condition. In the case of Fig. 6b', a shape-like morphology with rod-like and plate-like structure are obtained that corresponding to the formation under pH 2 condition. In addition, the elemental detection EDS analysis result presents in Fig. 7 confirming the existence of cerium and also oxygen on the galvanized steel surface after the immersion, that linking to the formation of the cerium-based conversion layer. Nervertheless, a hole-like structure is seen in Fig. 6c', relating to a smooth surface formed in pH 3-solution, compared to the high crystallinity obtained in the pH 2 (Fig. 6b'). When detected the change in the gloss retention on the surface before and after the pretreatment, the formation of this Ce-based layer diminues the gloss retention of initial galvaznied steel surface, from 640 GU (before pretraited) to 102 GU (for the case pretraited in pH 3) and 47 GU (for the surface pretraited in pH 2 solution). As the consequence, the pretreatment of galvaznied steel substrate in cerium-based solution at pH 2 obtains the lowest value in gloss retention. The decrease of the gloss retention value of galvanized steel surface leads to the development of the surface rugosity that can insprire in the reinforcement of adhesion properties between the galvaznied steel and the organic layer on top [19].

To clearly appreciate the reinforcement in adhesion behavior of cerium-based pretreatment layer with the top-

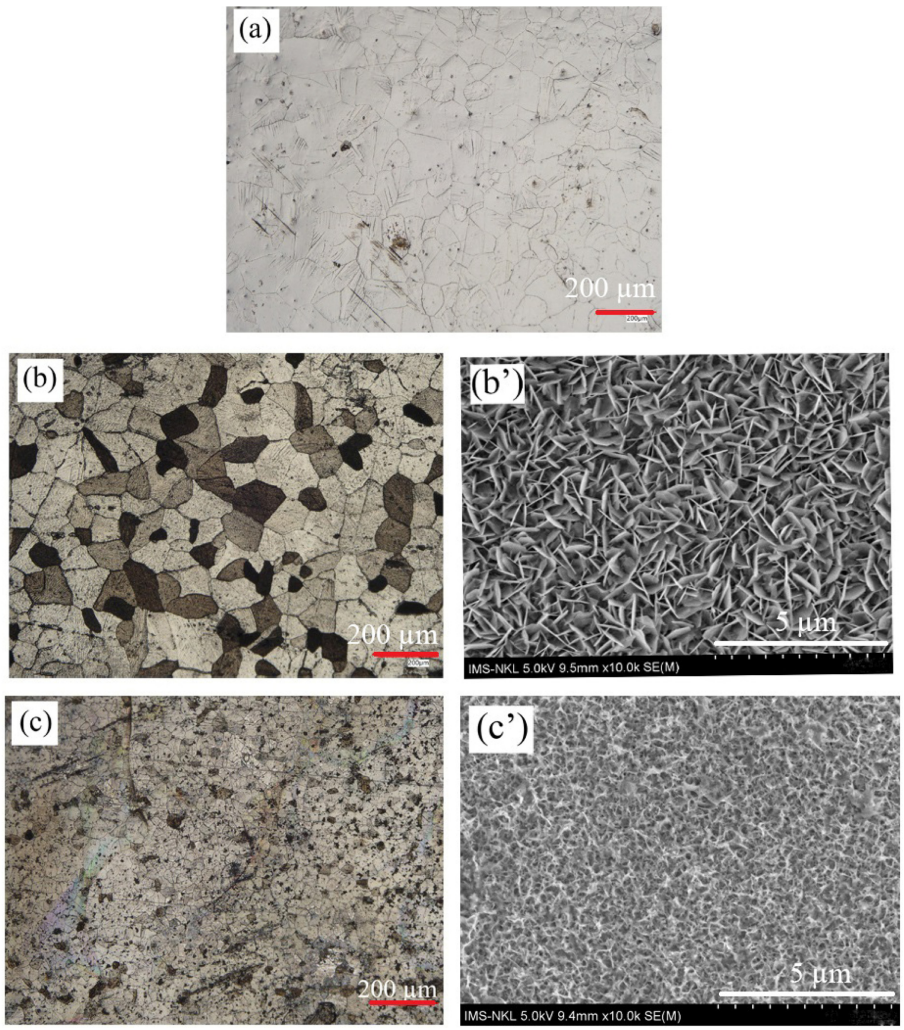

Fig. 6. Surface observation of galvanized steel substrate before (a) and after immersion in cerium-based solution under pH 2 (b, b') and pH 3 (c, c')

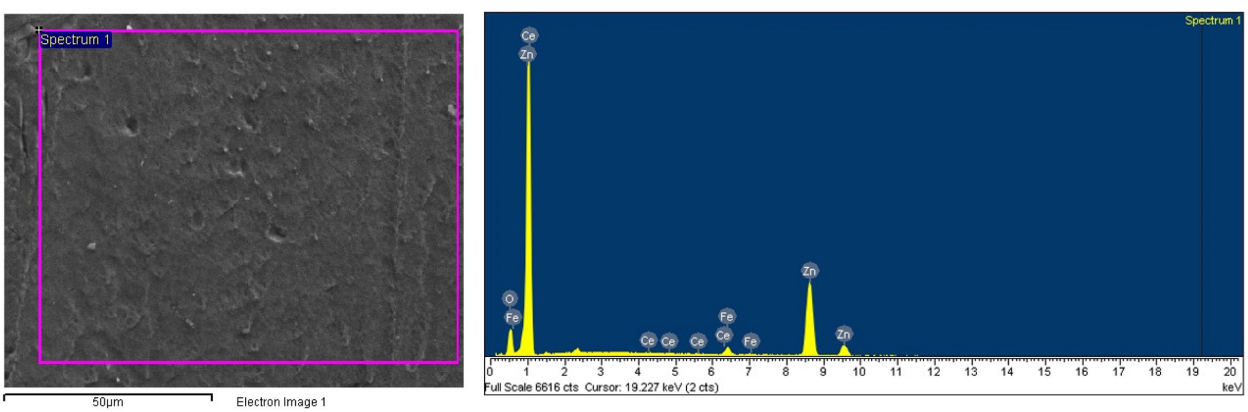

Fig. 7. EDS analysis detected on galvanized steel substrate after immersion in cerium-based solution under pH 2 (presented in Fig. 6.b, b')

coat organic layer, the pretreated and non-pretreated galvanized steel substrates were covered by a non-inhibitor epoxy (EP) layer and then examined the adhesion by pull-off test experiment. Fig. 8 presents the surface

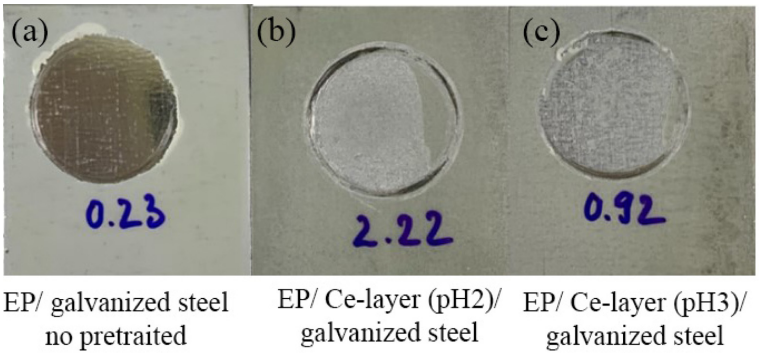

Fig. 8. Adhesion performance of EP/galvanized steel non pretreated (a) , EP/Ce-based layer (pH 2)/galvanized steel (b) , EP/ Ce-based layer (pH 3)/galvanized steel (c) after pull-off test followed ASTM D4541 standard

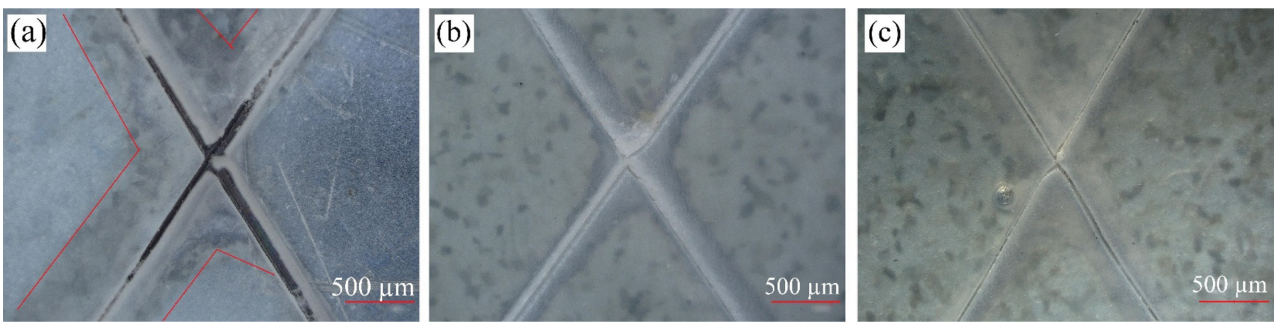

Fig. 9. Surface appearance of EP/galvanized steel non pretreated (a), EP/Ce-based layer (pH 2)/galvanized steel (b), EP/Ce-based layer (pH 3)/galvanized steel (c) after 14 days of salt spray test (ASTM B117 standard)

observation after the pull-off test followed by ASTM D4541 standard. As can be observed, for the neat epoxy layer covered on non-pretreated galvanized steel surface (Fig. 8a), the organic coating is totally removed from the metallic substrate after the adhesion test with the adhesion force of 0.23 MPa. When compared with the pretreated galvanized steel (in pH 3 solution)/ epoxy layer sample, the force recorded for the remove of the coating is 0.92 MPa (Fig. 8c) while this result is up to 2.22 MPa for the case of the pretreated galvanized steel (in pH 2 solution)/ epoxy layer sample (Fig. 8b). It is important to noted that in this case (pretreated under pH 2 condition), the organic coating was not completely removed from the surface. The significant increase in the adhesion capacity, especially higher than 10 times for the metallic substrate pre-immersed in the cerium-based solution at pH 2 related to the change in gloss retention of the substrate and also the high roughness of the Ce-based layer that were discussed in the previous section. In addition, the anti-corrosion properties of galvanized steel /epoxy coating are also reinforced as a result of the reinforcement in adhesion performance. Fig. 9 shows the surface appearance of pretreated and non-pretreated galvanized steel /epoxy layer after 14 days of salt spray test followed by ASTM B117 standard.

Regarding the surface observation obtained for the non-pretreated covered an epoxy layer (Fig. 9a), after 14 days of salt spray test, the corrosion products not only grow on the artificial scratch but also outside the cut. The permeation of water can be observed as the marked zone (in red line) linking to the attack of water through the cut to the intermediate layer under the organic coating so the adhesion between the epoxy layer and the galvanized steel was lost. When compared to the substrate pretreated with cerium-based conversion layer, Fig. 9b, 9c respectively, the permeated zone is limited. The white corrosion products on the scratch indicated the formation of Zn-compounds, as the action of sacrificial zinc coating layer. It must be noted that the dark spots observed in Fig. 9b and Fig. 9c point to the cerium-rich interlayer under the epoxy coating, not the corrosion products (as can be observed in Fig. 6). The Ce-based conversion coating as

the intermediate layer reinforces the adhesion between the organic layer and the metallic substrate, so the corrosive species cannot attack the coating through the cut. This reinforcement works not depending on the preparation pH condition.

5. Conclusions

This study focuses on the protective properties of cerium (III) oxide on the anticorrosion protection of galvanized steel substrate. The results highlighted the inhibitive ability of cerium (III) oxide:

- The EIS measurement also the polarization examination reveal the inhibition capacity of cerium (III) oxide on the electrolyte solution with a small content (0.05 wt%). Ce_2O_3 in this case works as a cathodic inhibitor, linking to the diminution of the current density in cathodic branch. The formation of a cerium-protective layer on the galvanized steel substrate was approved by FE-SEM and XRD analysis, which found a thick layer based on ZnO, $Zn_5(OH)_8Cl_2.H_2O$ and particularly $Ce_2(CO_3)_3.6H_2O$.

- In the light of these results, cerium (III) oxide particles were then used to prepare the cerium-based conversion layer as pretreatment layer. The influence of pH conditions was also examined. FE-SEM observations and EDS investigation were confirmed the formation of the cerium-based layer on the galvanized steel surface. This intermediated layer helps to reinforce the adhesion property between the organic coating and the metallic substrate (approved by ASTM D4541 pull off adhesion standard) by reducing the gloss retention of the initial surface and creating a surface more roughness, especially under pH 2 deposition preparation. As a result, the anticorrosion properties of epoxy layer/ Ce-based layer/ galvanized steel system are also reinforced.

Acknowledgments

The authors would like to thank ITT-VAST for financial support.

References

1. R. L. Twite and G. P. Bierwagen, Review of alternatives to chrome for corrosion protection of aluminum aerospace alloys, *Progress in Organic Coatings*, **33**, 91 (1998). Doi: https://doi.org/10.1016/S0300-9440(98)00015-0
2. R. Berger, U. Bexell, T. Mikael Grehk, and S.-E. Hörnström, A comparative study of the corrosion protective properties of chromium and chromium free passivation methods, *Surface and Coatings Technology*, **202**, 391 (2007). Doi: https://doi.org/10.1016/j.surfcoat.2007.06.001
3. K. Aramaki, Treatment of zinc surface with cerium (III) nitrate to prevent zinc corrosion in aerated 0.5 M NaCl, *Corrosion Science*, **43**, 2201 (2001). Doi: https://doi.org/10.1016/S0010-938X(00)00189-X
4. C. N. Panagopoulos, E. P. Georgiou, and C. Markopoulos, Corrosion and wear of zinc in various aqueous based environments, *Corrosion Science*, **70**, 62 (2013). Doi: https://doi.org/10.1016/j.corsci.2013.01.012
5. T. T. Nguyen, C. Arrighi, L. Dangreau, M. F. Gonon, A. T. Trinh, and M.-G. Olivier, Inhibitive effect of the Ce (III) chloride and nitrate on the corrosion resistance of Zn alloyed sacrificial coatings: Effect of alloying compounds of the sacrificial layer, *Electrochimica Acta*, **452**, 142296 (2023). Doi: https://doi.org/10.1016/j.electacta.2023.142296
6. C. Arrighi, T.T. Nguyen, Y. Paint, C. Savall, L.B. Coelho, J. Creus, M.-G. Olivier, Study of Ce(III) as a potential corrosion inhibitor of Zn-Fe sacrificial coatings electrodeposited on steel, *Corrosion Science*, **200**, 110249 (2022). Doi: https://doi.org/10.1016/j.corsci.2022.110249
7. V. Balaram, Rare earth elements: A review of applications, occurrence, exploration, analysis, recycling, and environmental impact, *Geoscience Frontiers*, **10**, 1285 (2019). Doi: https://doi.org/10.1016/j.gsf.2018.12.005
8. M. F. Montemor, A. M. Simões, and M. G. S. Ferreira, Composition and behavior of cerium films on galvanised steel, *Progress in Organic Coatings*, **43**, 274 (2001). Doi: https://doi.org/10.1016/S0300-9440(01)00209-0
9. M. A. Arenas and J. J. de Damborenea, Surface characterisation of cerium layers on galvanised steel, *Surface and Coatings Technology*, **187**, 320 (2004). Doi: https://doi.org/10.1016/j.surfcoat.2004.02.033
10. M. A. Arenas, C. Casado, V. Nobel-Pujol, and J. de Damborenea, Influence of the conversion coating on the corrosion of galvanized reinforcing steel, *Cement & Concrete Composites*, **28**, 267 (2006). Doi: https://doi.org/10.1016/j.cemconcomp.2006.01.010
11. W. Pinc, S. Geng, M. O'Keefe, W. Fahrenholtz, and T. O'Keefe, Effects of acid and alkaline based surface preparation on spray deposited cerium based conversion coatings on Al 2024-T3, *Applied Surface Science*, **255**, 4061 (2009). Doi: https://doi.org/10.1016/j.apsusc.2008.10.110

12. Z. Mahidashti, T. Shahr, and B. Ramezanzadeh, The role of post-treatment of an ecofriendly cerium nanostructure conversion coating of green corrosion inhibitor on the adhesion and corrosion protection of the epoxy coating, *Progress in Organic Coatings*, **114**, 19 (2018). Doi: https://doi.org/10.1016/j.porgcoat.2017.09.015
13. B. Ramezanzadeh and M.M. Attar, An evaluation of the corrosion resistance and adhesion properties of an epoxy-nanocomposite on a hot-dip galvanized steel (HDG) treated by different kinds of conversion coatings, *Surface and Coatings Technology*, **205**, 4649 (2011). Doi: https://doi.org/10.1016/j.surfcoat.2011.04.001
14. F. Deflorian, M. Fedel, S. Rossi, and P. Kamarchik, Evaluation of mechanically treated cerium (IV) oxides as corrosion inhibitors for galvanized steel, *Electrochimica Acta*, **56**, 7833 (2011). Doi: https://doi.org/10.1016/j.electacta.2011.04.014
15. U. Eduok, O. Faye, A. Tiamiyu, J. Szpunar, Fabricating protective epoxy-silica/CeO_2 films for steel: Correlating physical barrier properties with material content, *Materials and Design*, **124**, 58 (2017). Doi: http://doi.org/10.1016/j.matdes.2017.03.062
16. G. Cheng, Z. Song, Y. Mao, J. Zhang, K. Wang, H. Li and Z. Huang, Effect of Ce_2O_3 phase transition on the catalytic oxidation for toluene over CeO_2 catalysts, *Fuel*, **368**, 131641 (2024). Doi: https://doi.org/10.1016/j.fuel.2024.131641
17. T. T. Thai, A. T. Trinh, T. T. T. Pham, X. H. Nguyen, G. V. Pham, and T. X. H. To, Corrosion inhibition of Galvanized steel by Cobalt (II) nitrate, *e-Journal of Surface Science and Nanotechnology*, **19**, 48 (2021). Doi: https://doi.org/10.1380/ejssnt.2021.48
18. Y. Meng, L. Liu, D. Zhang, C. Dong, Y. Wan, A. A. Volinsky and L.-N. Wang, Initial formation of corrosion products on pure zinc in saline solution, *Bioactive Materials*, **4**, 87 (2019). Doi: https://doi.org/10.1016/j.bioactmat.2018.08.003
19. T. T. Thai, M.-E. Druart, Y. Paint, A. T. Trinh, and M.-G. Olivier, Influence of the sol-gel mesoporosity on the corrosion protection given by an epoxy primer applied on aluminum alloy 2024-T3, *Progress in Organic Coatings*, **121**, 53 (2018). Doi: https://doi.org/10.1016/j.porgcoat.2018.04.013